Adhesion of micro-organisms to bovine submaxillary mucin coatings: Effect of coating deposition conditions

Ibraheem A. Bushnak,[a] Fatima H. Labeed,[b] Richard P. Sear,[a] and Joseph L. Keddie[a]

[a]*Department of Physics, University of Surrey, Guildford, Surrey, GU2 7XH UK;*

[b]*Centre for Biomedical Engineering, University of Surrey, Guildford, Surrey, GU2 7XH UK*

The adhesion of *Staphylococcus epidermidis, Escherichia coli,* and *Candida albicans* on mucin coatings has been evaluated to explore the feasibility of the coating to increase the infection resistance of biomaterials. Coatings of bovine submaxillary mucin (BSM) were deposited on a base layer consisting of a poly(acrylic acid-*b*-methyl methacrylate) (PAA-*b*-PMMA) diblock copolymer. This bi-layer system exploits the mucoadhesive interactions of the PAA block to aid the adhesion of mucin to the substrate, whereas the PMMA block prevents the coating's dissolution in aqueous environments. The thickness of the mucin coating was adjusted by varying the pH of the solution from which it was deposited. Thin mucin coatings decreased the numbers of bacteria but increased the numbers of *C. albicans* adhering to the copolymer and control surfaces. Increasing the mucin film thickness resulted in a further lowering of the number density of adhering *S. epidermidis* cells, but it did not affect the number density of *E. coli*. In contrast, the *C. albicans* number densities increased with an increased mucin thickness.

Keywords: *Mucin, poly(acrylic acid), mucoadhesion, Staphylococcus epidermidis, Escherichia coli, Candida albicans, coatings. Bayesian statistics*

Introduction

There is a need for lubricating coatings for cardiovascular stents (Singh et al. 2007) and urinary catheters (Tunney and Gorman 2002) to aid their insertion and effectiveness. Hydrophilic polymer layers have been found to be sufficiently lubricious for these

applications while also being able to reduce bacterial adhesion and associated contaminants that lead to infections (Tunney and Gorman 2002). There is therefore interest in developing ways to deposit hydrophilic polymer coatings and to evaluate their properties. In this present work, the naturally-occurring macromolecule, mucin, is used to make coatings.

Our inspiration has come from previous studies showing that physisorbed mucin layers can suppress the adhesion of some bacterial species on various polymer surfaces (Shi and Caldwell 2000, Shi et al 2000). The reduction in bacterial adhesion was attributed to the reduced hydrophobicity of the surfaces resulting from coverage by the physisorbed mucin. In this previous work, neither the deposition method nor the thickness of the mucin coatings were varied.

Mucin is a natural polymer that belongs to the glycoprotein family (Peppas and Huang 2004). There are two types of mucins: membrane-bound mucin and secretory mucin. They have similar structure with minor differences, and they work together to form the mucus protective layer (Strous and Dekker 1992, Bansil et al 1995). Mucin makes up 5% by weight of the mucus secretions in the human body (Malmsten et al 1992). Mucus is secreted by the luminal surfaces of the epithelial organs to form a physical protective barrier against viral and bacterial attachment, abrasion and diluting chemicals (*e.g*. stomach acid) (Shi et al. 2000). It also plays a part in the cellular signaling mechanisms and cell-cell interactions. Other functions of mucus are lubrication and pH regulation (Strous and Dekker 1992).

Mucins are complex glycoproteins made up of a peptide backbone with bare and highly glycosylated blocks. The long linear peptide backbone makes up between 20 to 50% of the mucin molecule, and the remaining 50 to 80% of the molecule consists of carbohydrate side chains (Malmsten et al 1992, Sheehan et al. 1986). The carbohydrate side chains are attached to the peptide core in a “bottle brush” configuration, and they

consist primarily of acetyl-D-galactosamine, galactose, fucose, sialic acid and acetyl-D-glucosamine.

The peptide backbone is made up of several repeats of amino acids arranged into two main distinct regions: highly glycosylated and bare regions (Bansil and Turner 2006). The highly glycosylated regions are rich in serine, threonine and proline and the bare regions are rich in cystine.

Mucin has an overall negative charge in basic and neutral solutions, which diminishes as the pH decreases below pH 4 as it gets closer to the isoelectric point (p*I*) (Malmsten et al 1999). In general, the p*I* of mucins can range between 4.7 and 2, depending on the mucin's origin and method of preparation (Prescott et al 1993, Hancock and Poxton 1988). The p*I* of bovine submaxillary mucin (BSM), which is studied herein, has been determined to be 3 (Perez and Proust 1987). Below this point, the mucin molecule becomes protonated and loses its negative charge (Prescott et al. 1993).

The peptide backbone is hydrophobic and adheres to hydrophobic surfaces. However, the carbohydrate side chains are hydrophilic and have a large charge density due to the presence of sialic acid and sulfate residues. Hence, mucin molecules are amphiphilic (Sheehan et al 1986). When absorbed on a hydrophobic surface, mucin molecules make it strongly hydrophilic, making them a good candidate material for antifouling coatings (Shi et al 2000).

Micro-organism adhesion: process and significance

Bacterial adhesion and contamination is one of the leading problems in the medical, dental and food industries. In medical applications, surface-associated bacterial infections are the primary cause of device failure (Rutter al. 1984). The process of bacterial adhesion to any surface is dictated by many variables, including the bacterial

species, the surface properties and structure of the biomaterial and bacteria, and the surrounding environment (Rutter et al. 1984). Understanding these variables will allow a fuller understanding of the adhesion mechanism.

Cellular adhesion, in general terms, always starts with long-range, non-specific, reversible interactions between the unicellular organism and the substrate surface in a process termed the "docking" stage. Electrostatic and van der Waals forces are the main long-range interactions. These interactions depend on the physical and chemical surface properties of the organism and the substrate, as well as the medium (Gingell and Vince 1980). Once the cell is in close proximity to the surface, short-range, and irreversible interactions, such as receptor-ligand binding events, occur during what is called the "locking" stage (Rutter et al. 1984, Gingell and Vince 1980, Wardell 1988). Here, we will only consider adhesion during the first two hours of bacterial exposure. Over longer periods, microorganisms can show a range of complex behaviours, such as the formation of structured biofilms with large aggregates of many cells (Mack et al. 2004, Allegrucci et al. 2006).

Aims of the work

In this present work, robust bovine submaxillary mucin (BSM) coatings are attached to substrates through the use of a "primer" layer to ensure permanent attachment. This layer consists of a diblock copolymer of poly(methyl methacrylate) (PMMA) and poly(acrylic acid) (PAA). Mucin has been shown to undergo attachment to PAA via hydrogen bonding interactions (Patel et al. 2003, Nikonenko et al. 2009), and hence BSM is bonded to this copolymer. Indeed PAA polymers have been developed as mucoadhesive films for drug delivery to mucosal tissues (Dubolazov et al. 2006). In the copolymer used here, the PMMA block ensures that the film does not dissolve in water so that it is able to facilitate the physisorption of the mucin layer from

aqueous solutions.

The adhesion of two bacterial microorganisms - *S. epidermidis* and *E. coli* - and a fungal microorganism *C. albicans* on the surfaces of BSM were investigated. (Whereas the first of these bacteria species is gram-negative, the second is gram-positive.) These organisms were chosen as they were linked with catheter-associated urinary tract infections (CAUTIs) (Tenke et al. 2004). Previous work has found that bacteria colonize inside and outside of an indwelling catheter and create a biofilm (Wong and Hooton 1981). Hydrophilic polymers, antibiotics, heparin (Tenke et al. 2004, Wong and Hooton 1981) and silver alloys (Davenport and Keeley 2005) have all been used previously in coatings of catheters in an attempt to prevent CAUTIs. It was hypothesized in this work that, because of their hydrophilicity, mucin coatings will be able to prevent the *initial* (docking) stage of adhesion of some bacterial and fungal species associated with CAUTIs. This work specifically investigates the use of mucin as a coating material that is resistant to the adhesion occurring within the first two hours of exposure. Furthermore, the natural lubricity of mucin coatings is expected to offer additional benefits in catheter insertion (Tunney and Gorman 2002).

Materials and methods

Surface preparation

Polished <100> silicon were used as substrates, because of their suitability for ellipsometry measurements. As-received wafers were cut and coated with poly(methyl methacrylate) (Polymer Laboratories UK, number-averaged molecular weight of M_n = 80,000 g/mol) as a control surface *or* with a PAA-*b*-PMMA diblock copolymer (Polymer Source, Quebec, Canada, Cat. No. P2993-AAMMA; PAA: M_n = 28,000 g/mol; PMMA: M_n = 10,000 g/mol; polydispersity of M_w/M_n = 1.14) as a base layer for mucin coatings. Polymer films were spin-coated from 0.5 w/w% solutions onto 2 cm x

2 cm silicon <100> substrates at a rate of 2000 rpm for 4 seconds. Toluene was used as the solvent for PMMA, and tetrahydrofuran was used for PAA-*b*-PMMA. Then the films were annealed in a vacuum oven at 120 ºC for two hours to remove residual solvent and to allow the films to relax (Richardson et al. 2004). This technique yielded smooth films with thicknesses ranging between 15 and 25 nm.

Mucin adsorption

BSM (Sigma Aldrich, Catalogue No. M 3895) was used as received. Mucin macromolecules have a molecular weight in the range between 0.5 and 40×10^6 Daltons and a persistence length of 100 nm (Bloomfield 1983). BSM solutions were prepared in phosphate buffer solution, PBS (at a pH of 7), at a concentration of 1 mg/ml. Silicon substrates and polymer-coated substrates were incubated in the mucin solution for 24 hours while shaking to allow the adsorbed layer to reach equilibrium (Shi and Caldwell 2000). In some experiments, the pH of the mucin solution was adjusted to 3 through the addition of hydrochloric acid or adjusted to 10 through the addition of sodium hydroxide. After mucin adsorption, the samples were rinsed three times with 25 ml of PBS at a pH of 7, to rinse off unbound mucin. Next, the samples were left in a desiccator with silica gel to allow the films to dry before thickness measurements.

Film thickness measurements

Ellipsometry is a non-invasive optical technique that uses the reflection of polarised light to measure the refractive index profile of a sample and thereby to provide thickness measurements of thins films. The technique depends on the fact that the polarization of the light changes when it is reflected from an interface, because of the difference in the refractive index at the interface. It is a very accurate technique that can be used to measure film thicknesses as low as 1 nm (Keddie 2001).

Fresnel reflection coefficients are defined for the two linear polarization states, in the plane of reflection (R_p) and perpendicular to the plane of reflection (R_s). The ratio

of the Fresnel coefficients (R_p/R_s) determines the complex parameter ellipticity (ρ). In turn, the ellipsometry parameters, ψ and Δ are found through the relation:

$$\rho = \frac{R_p}{R_s} = \tan \psi e^{i\Delta}$$

The two ellipsometry parameters are measured during an experiment and used to determine the unknown parameters in the system under investigation. The thicknesses and refractive indices of the films (spin-cast and adsorbed layers) were determined using a variable-angle spectroscopic ellipsometer (J.A. Woollam Co., Inc., Lincoln, NE, USA) in air. The angle-of-incidence was selected in the range between 64° and 75°, depending on the substrate and the particular system, and the wavelength ranged across the visible region from 400 to 800 nm. The central area of the film was probed in all experiments. Spectra were analysed using commercial software (WVASE 32, J.A. Woollam Co., Inc.) following the procedure described previously (Nikonenko et al. 2009).

All films were stored in a desiccator prior to their analysis in order to dehydrate them and to ensure reproducibility of the thickness measurements. (The copolymer thickness was found to increase with the relative humidity, but the initial thickness was recovered when placed in a low humidity atmosphere.)

Contact angle analysis

The contact angles of sessile drops of de-ionized water on the surfaces of PMMA and PAA-*b*-PMMA and on adsorbed mucin layers were determined with a high-definition camera and image analysis software (Krüss GmbH, Germany).

Micro-organism adhesion assay

Freeze-dried cultures (obtained from ATCC®, LGC, Teddington, UK) were re-hydrated and grown in liquid growth medium. The growth medium and conditions that were recommended by distributor were used, as follows. *S. epidermidis* (ATCC® 14990) and

E.coli (ATCC® 39403) strains were grown in tryptic soy broth at 37 °C. *C. albicans* (ATCC® 38289) was grown in yeast mold broth at 25°C. The cultures were incubated for 24 hours under the appropriate conditions.

The mucin-coated and the uncoated surfaces were placed in multi-well dishes, and the wells were filled with 5 mL of cell suspension at a concentration of $5x10^7$ cell/mL. The surfaces were left to incubate in the bacterial cell suspensions while shaking for two hours at 37 °C. In the case of the *C. albicans,* the surfaces were incubated in the suspension at 25 °C for two hours while shaking to prevent sedimentation. This time period was chosen to represent the initial stage of adhesion (the docking stage). The surfaces were then rinsed three times with 25 mL of PBS to remove all the unattached bacteria. The cells were fixed on the surface using glutaraldehyde solution, following the procedure described elsewhere (Shi et al. 2000). Three replicate substrates were incubated for each sample type, in order to take into account variability between the substrates. Three different randomly-chosen positions on each of the substrates were imaged under an optical microscope, and cells were counted within a field of view of $6.2x10^{-4}$ cm^2. Cell densities were calculated as the number of observed cells per unit area. Each experiment was conducted three times using new bacterial cultures.

Analysis of cell counts

For each substrate, 27 measurements of the cell density in total were obtained from three randomly-selected areas on each of three substrates in three repeat experiments. There is some relatively small amount of scatter in the number of cells counted in each set of 27 measurements. Bayesian statistical analysis of the 27 measurements was employed to obtain the best estimate of the true average cell density on each type of substrate. For an introduction to Bayesian statistics, see Mackay (2004) and DeGroot and Schervish (2002).

Now, before the measurements are made, we do not know the true average cell

density ρ, nor do we know the functional form or extent of the scatter. For simplicity, we assume a Gaussian distribution around the true average ρ with a standard deviation σ. Then if the true average cell density is ρ, the probability of measuring a cell density m is given by

$$p(m \mid \rho,\sigma) = \exp\left[-(m-\rho)^2/(2\sigma^2)\right]/(2\pi\sigma^2)^{1/2}.$$

Now, we wish to obtain the best estimates for ρ and σ. We start with a conservative prior density function, $p_0(\rho, \sigma)$, in which both ρ and σ are uniformly distributed anywhere in the range from 0 to 10^7 cells/cm^2. Bayes' theorem then tells us that the probability density function for true cell density ρ and the scatter about this in individual measurements, σ, is

$$p(\rho,\sigma) \propto p_0(\rho,\sigma)\prod_{i=1,27} p(m_i \mid \rho,\sigma).$$

Here the product is over all 27 cell density measurements for the surface type, m_i, $i=1$-27. The proportionality constant means that we normalise after applying Bayes' theorem. If we integrate the probability density function $p(\rho, \sigma)$ over σ, we obtain the required probability density for the true average cell density on a particular substrate, $p(\rho)$. This probability density provides the most likely value of the true average density of cells. The width of $p(\rho)$ defines the extent of uncertainty as to this value. Furthermore, if two $p(\rho)$ probability density functions do not have significant overlaps, then the adhesion to the two substrates is certain to be significantly different. We have verified that varying the prior distribution has little effect on the ρ obtained. Also, performing the analysis not for the complete set of the data - but for subsets of it - shows no significant systematic variation between one experiment and another.

Results

Film characterization

The thicknesses of the native silicon oxide layers and the deposited polymer thin films were determined with ellipsometry. Values are listed in Table 1. After these measurements, mucin was adsorbed on the various substrates from solutions at a pH of either 3, 7 or 10. The thicknesses of the adsorbed mucin layers are presented in Table 1. The thicknesses of the mucin layer on silicon and PMMA range between 2.4 and 3.0 nm regardless of the pH of the solution from which they were adsorbed. The mucin layer thicknesses adsorbed on the copolymer PAA-b-PMMA, however, are 10 nm thicker when the pH of the mucin solution was 3 in comparison to the thickness when the pH was 7.

The higher mucin thickness on the PAA-b-PMMA surfaces can be explained by hydrogen bonding between poly(acrylic acid) and mucin molecules. Previous studies (Patel et al 2003, Park and Robinson 1987, Cao et al 1999) have shown that, the activation of the mucin's carboxylic groups (COOH) below its isoelectric point (pH <4) creates more hydrogen bonds between the mucin's sialic groups and the carboxylic acid groups in PAA. Consequently, more mucin is attached to the copolymer surface and thicker layers are created in comparison to what is found at neutral and basic pH solutions. Silicon and PMMA do not participate in pH-dependant hydrogen bonding. This result is evident by the constant mucin thickness on silicon and PMMA for the all pH values 10, 7, and 3, as seen in Table 1.

As a means of comparing the relative hydrophilicity of the polymer surfaces, measurements of the contact angle of sessile drops of water were made. The results in Table 2 show that the contact angle on PMMA films is 69.4° ±0.2° in comparison to PAA-*b*-PMMA on which it is initially 49°±1°, indicative of a more hydrophilic surface. Over time, the copolymer swells with water and it becomes more hydrophilic. The contact angle decreases to an average of 27° ±3°. The contact angle for bare silicon surface was intermediate between the two polymers with a value of 62.3° ±1.3°.

Mucin adsorption onto the PMMA surfaces imparts hydrophilicity, as indicated by the decrease in the water contact angle, with a slightly lower value observed when the mucin was adsorbed from a solution with a pH of 7 compared to a pH of 3. The standard deviation on the measurements reflects the non-uniformity of the surfaces at the sub-μm scale, leading to variations in the replicate experiments. In general, the contact angle showed greater variability on the mucin-coated PMMA compared to the mucin-coated copolymer. This variability is likely to result from heterogeneity in the coverage of the mucin on the more hydrophobic PMMA, whereas the muco-adhesive interactions with the PAA block in the copolymer result in more homogeneous coverage.

Mucin adsorption on the PAA-*b*-PMMA surface has a different effect. When mucin is adsorbed at a pH of 7, the contact angle is the same as on the hydrated copolymer surface. On the other hand, after adsorption of mucin at a pH of 3, the mucin increases the hydrophilicity of the surface and reduces the contact angle to 22.6°, which is the lowest of all the surfaces. Note that the measurements were made on mucin layers that had been dried in a desiccator. Hence, the contact angles are higher than reported elsewhere for mucin films (Shi et al 2000). After the mucin films are hydrated, the surfaces are fully wetted by water, and contact angles cannot be measured.

S. epidermidis adhesion

The representative images in Figure 1 show adhered cells of *S. epidermidis* on uncoated and mucin-coated surfaces of the control materials: silicon and PMMA. *S. epidermidis* is clearly visible in the images as individual spherical cells or as small clusters of five to ten cells. Figures 1a and 1c of the bare silicon and PMMA surfaces have large numbers of bacteria adhering to them (6.9×10^6 bacteria/cm^2 and 2.5×10^6 bacteria/cm^2, respectively). When these two surfaces are coated with mucin, many fewer cells are

adsorbed. See Figures 1b and 1d, Figure 2, and Table 3. The curve of the probability density function for cell adhesion to Si/mucin (PMMA/mucin) in Figure 2 is well separated from that for Si (PMMA), so we conclude that the effect of mucin coating is easily large enough that the inevitable noise arising from the variability in the number of cells from area to area does not obscure it. This conclusion can also be drawn from Table 3, which presents estimates for the true cell density and the uncertainty in this number.

In comparison to the bare Si and PMMA control surfaces, fewer *S. epidermidis* cells are adsorbed on the bare PAA-b-PMMA surface, as shown in Figure 3a. The cell counts are reduced further when the copolymer is coated with mucin (Figures 3b and 3c). The lowest number of cells is adsorbed on the thicker mucin coating on the copolymer, which was deposited at a pH of 3. Note that the density of *S. epidermidis* cells there is over one hundred times lower than on the Si substrate, see Table 3. The thinner mucin coating (deposited at a pH of 7) has statistically significantly more adhered cells, in comparison, but only by a factor of approximately two.

The poly(acrylic acid) block of the copolymer is polar and has the ability to absorb water and to swell, reducing the net hydrophobicity of the surface as seen from the water contact angle measurement of 40.0±0.8°. The extension of hydrophilic chains into the solution might play a role in minimizing the contact time of bacteria to the surface, thus reducing the chances of the initial stage of adhesion. Adsorbing a mucin layer on top of the copolymer making it resistant to bacterial adhesion, see Table 3 and Figure 2.

E. coli adhesion

The images in Figure 4 show examples of the adhered *E. coli* cells to both uncoated and mucin-coated silicon and PMMA surfaces. The cells in Figure 4 appear as individual

cylindrical cells or as aggregates. The aggregates only appear on the surface of the silicon substrate as seen in Figure 4a, whereas individual cells are found on the other surfaces. The adhered cells on bare silicon and PMMA are similar in number (about $1x10^6$ bacteria/cm^2), as counted from areas such as are shown in Figures 4a and 4c. After coating with mucin, there is a reduction in cell numbers, which is particularly apparent for PMMA (Figures 4b and 4d). The *E. coli* cell density measurements are presented in Figure 5. These results show a statistically-significant reduction in *E. coli* cells adhering to the mucin-coated surfaces.

The number density of cells adhering to the PAA-*b*-PMMA copolymer was reduced when the copolymer was coated with mucin. (Micrographs are not shown here.) However, for *E. coli*, unlike the results for *S. epidermidis,* the thicker mucin layer deposited at a lower pH (3) did not result in a significantly lower amount of cell adhesion in comparison to the thinner layer deposited at a pH of 7. For details, compare the last two rows of Table 3. Note also the significant overlap of the probability distributions of the cell density for the thin and thick mucin coatings seen in Figure 5.

C. albicans adhesion

In comparison with the results from the bacterial adhesion experiments, the mucin coating appears to be less effective in suppressing the adhesion of the yeast *C. albicans*. The representative surfaces shown in Figure 6 indicate that the yeast cells adhere to all of the surfaces without obviously apparent differences between the mucin-coated and uncoated surfaces. The only exception is found on the bare PAA-*b*-PMMA surfaces, shown in Figure 6e, which has the lowest number of *C. albicans* cells on the surface. This conclusion is more evident when looking at the cell counts presented in Figure 7, where it is clear that only the bare PAA-b-PMMA exhibits some suppression of the number of adhered *C. albicans* cells.

Discussion

Interpretation of bacterial adhesion results

Quantitative analysis of the images shows that the mucin-coated Si, PMMA and PAA-*b*-PMMA exhibited a reduction in the numbers of adhering bacteria when compared to the uncoated surfaces. This reduction is attributed to an increase in the hydrophilicity of the surfaces caused by the mucin coating. Coating with mucin yielded a reduction of more than 70% for both types of bacteria and for silicon, PMMA and copolymer surfaces, except for the case of *E. coli* on silicon, which had a 49% reduction. See Table 3. The lower reduction on the mucin-coated Si surfaces for the *E. coli* can be attributed to a patchy coverage of mucin on that surface (Shi and Caldwell 2000, Shi et al 2000).

Although the hydrophobicity of bacteria depends on the species, the strain and the conditions of growth, there are suggestions that the degree of hydrophobicity of *E. coli* is lower than other bacterial species (Rosenberg 1988). Hydrophobicity tests have found that *E. coli* is significantly less hydrophobic than *S. epidermidis* (Gilbert et al. 1991). This finding can explain why in our study more *S. epidermidis* adhered to the hydrophobic Si and PMMA substrates in comparison to *E. coli*.

The mucin coating reduced the numbers of *E. coli* by roughly 70%, whereas the numbers of *S. epidermidis* were reduced by 90%, suggesting that mucin coating is more effective in suppressing *S. epidermidis* adhesion in comparison to *E. coli*. The presence of the pili and flagella on the surface of the *E. coli* cells (Rutter et al 1984) might give it an advantage when it comes to adhering to the mucin-coated surfaces. Furthermore, Vacheethasanee *et al*. (1998) showed that *S. epidermidis* is influenced more by the hydrophobicity of a surface than by its charge. Their findings support the idea that the reduced numbers of adhered *S. epidermidis* when there is a mucin layer is a result of the reduced hydrophobicity.

Ellipsometry provides a measure of only the *average* thickness of a film. It is likely that the mucin coatings are non-uniform at the molecular level. The mucin coating on PAA-*b*-PMMA was measured to be twice as thick as that on Si and PMMA. It is likely that the ultrathin mucin layers on Si and PMMA are patchy. In this latter case, the mucin is physisorbed on the substrate surface, but the layer is unlikely to be continuous at the molecular level. Our results indicate that a thicker, more uniform mucin coating is more effective in reducing bacterial adhesion than a thinner non-uniform mucin coating.

Figure 8 illustrates the correlation between the thickness of mucin layer and the adherence percentage, which is calculated from the ratio between the cell numbers on the mucin-coated surface and the numbers on the same bare surface. Figure 8 shows that as the thickness of the mucin layer is increased, via hydrogen bonding between mucin and the PAA copolymer (Nikonenko et al. 2009), a further reduction in the numbers of *S. epidermidis* cells is observed. This reduction obtained from the thicker mucin coatings in comparison to the thin coating is calculated to be 43%. This effect can be partially attributed to the increased hydrophilicity of the thicker mucin layer, as seen from the contact angle measurements. A likely explanation is that the thicker mucin coating, prepared at a pH of 3, is denser at the molecular level and has no bare patches. The hydrogen-bonding between the mucin and the PAA blocks of the copolymer ensures that a continuous coating is achieved. This coating is therefore more effective in suppressing bacterial adhesion. Defects and bare patches that are present in thinner films could enable a means of attachment.

Furthermore, as the mucin thickness increases, the physical and chemical properties might change slightly because of the increased number of attached mucin molecules per unit area. In a monolayer of mucin, the macromolecules can re-orient themselves so that their hydrophobic components are facing a hydrophobic substrate

and its hydrophilic components facing a hydrophilic media (Shi et al. 2000, Shi and Caldwell 2000). The re-orientation is dependent on the substrate hydrophobicity and the media. As the thickness of the mucin layer increases, the fraction of any bare surface will decrease towards zero. Furthermore, with increasing thickness, the top mucin layer might reorient differently, such as extending more into the media. In a monolayer, a greater fraction of the molecules could be attached to the substrate. Hence, there could be differences in charge density distribution and hydrophobicity between a molecular monolayer and a thicker film. These differences could explain the reduced *S. epidermidis* adhesion.

On the other hand, counts of *E. coli* cells showed a major reduction in the numbers on the mucin-coated copolymer compared to the bare PAA-b-PMMA (78%), as seen in Figure 5, but there was no further reduction in the numbers of *E. coli* cells when the thickness of the mucin coating was increased. The adhesion percentage in Figure 8 is not changed when the mucin coating thickness is varied. There could be many explanations, among which is the presence of adhesive fimbriea on the surface of *E. coli*, as was mentioned previously. These adhesive organelles have been observed to facilitate the adhesion of *E. coli* to intestinal mucosa by anchoring cells to the mucus surface followed by cell aggregation on the anchored cells (Cruz Ramos et al 2004, Girón et al 2002). Thus, the *E. coli* could have an adhesion mechanism on the mucin-coated surfaces, which is analogous to what is found *in vivo*, and which is not operative for the *S. epidermidis*.

Interpretation of yeast adhesion results

The observed results in Figure 7 indicate that the yeast cells were able to adhere to the mucin-coated surfaces. In the case of PMMA, the mucin coating had no effect on the suppression of *C. albicans* adhesion. Moreover, the numbers of *C. albicans* adhering to

the bare PAA-*b*-PMMA surface were less than that on the mucin-coated PAA-*b*-PMMA surface, which leads us to conclude that *C. albicans* exhibited some affinity to mucin.

Results in Figure 8 suggest that as the thickness of the mucin layer increases, the adherence percentage increases. It has been reported that the cell wall of *C. albicans* contains residues of sialic acid that contribute to the cells' overall electrostatic potential (Hobden et al 1995). Reports of the degree of *C. albicans'* outer surface hydrophobicity vary greatly; whereas some studies have found it to be hydrophobic (Hobden et al 1995, Hazen 1989), others report that it was slightly hydrophilic (Klotz et al 1985). It is been reported that *C. albicans* is capable of producing a surfactant that makes the cell surface more hydrophobic (Sundstrom 1999). These surfactants are either cell-wall associated or excreted to the cells' surroundings to aid in the adhesion process. The inconsistent results in the literature might be explained by the yeast's capability of changing its surface hydrophobicity in response to its environment. If the yeast changed its surface hydrophobicity to become more hydrophilic, this might explain the large numbers present on the mucin.

Summary and Conclusions

An adsorbed mucin layer on silicon and PMMA surfaces reduces the number of *S. epidermidis* cells adhering to them. This result shows the effectiveness of a mucin coating in suppressing bacterial adhesion even at low thickness values. A PAA-*b*-PMAA copolymer coating also showed bacterial adhesion resistant properties, due to its hydrophilicity, when compared to the PMMA surface.

A thin mucin coating on PAA-*b*-PMMA reduced the number of *S. epidermidis* adhering when compared to the bare PAA-*b*-PMMA surface. Increasing the mucin layer thickness on PAA-b-PMMA, by depositing it from a solution at a pH of 3, further reduced the number of *S. epidermidis* adhering cells when compared to the thin mucin

coating. The thicker coating is strongly adsorbed on the substrate via hydrogen bonding, and it acts as a robust hydrophilic barrier against bacterial adhesion. It is likely that the thicker mucin coating is continuous and defect-free at the molecular level, unlike the situation for the other coatings.

The number of adhering *E. coli* cells was similarly reduced after coating silicon, PMMA, and PAA-*b*-PMMA with mucin. Coatings on the copolymer were less effective, however, in reducing the adhesion of *E. coli* in comparison to *S. epidermidis*, when considered as a percentage reduction of the number densities on the uncoated surface. The mucin coating on PAA-*b*-PMMA reduced the adhesion of *E. coli* by 84%.

In contrast, the mucin coating on silicon and PMMA was not effective in reducing the number densities of adhered *C. albicans* cells. Furthermore, the thicker mucin coating on PAA-*b*-PMMA *increased* the densities by 77% compared to the bare PAA-*b*-PMMA surface. This result indicates that even at our short incubation times of two hours, *C. albicans* has an affinity for the mucin coating. Landry *et al.* (2005) used much longer incubations times in their study of the bacterium *Pseudomanas aeroginosa*. They found that on mucin-coated surfaces this bacterium formed large aggregates of many cells. Both *C. albicans* and *P. aeroginosa* commonly affect mucus-covered tissues, and so it is perhaps not surprising that mucin coatings are ineffective in preventing adhesion. Indeed our uniform and controlled coatings may be useful in the systematic study of this phenomenon. For this class of organism, our synthetic copolymer surfaces may be most resistant to adhesion, although experiments with much longer incubation times are required to study this aspect. Our mucin coatings may be best suited to resist adhesion by microorganisms that have not evolved to infect naturally mucin-coated tissues.

Acknowledgements

We dedicate this paper to Dr. Tony Chamberlain (University of Surrey), who

contributed to the very early stages of the work but passed away before it was complete. I.A.B. acknowledges a PhD scholarship from the Ministry of Higher Education of Saudi Arabia. We thank Dr. Noel Wardell (University of Surrey) for providing protocols for the bacteria, Dr. Henry Fatoyinbo (University of Surrey) for assistance with the bacteria cultures, Dr. Nataliya Nikonenko (Belarus Academy of Sciences) for useful discussions, and Mrs. Violeta Doukova (University of Surrey) for general laboratory assistance.

References

Allegrucci M, Hu FZ, Shen K, Hayes J, Ehrlich GD, Post JC, Sauer K. Phenotypic Characterization of *Streptococcus pneumoniae* biofilm development. 2006. J. Bacteriol. 188:2325-2335.

Bansil R, Stanley E, LaMont JT. 1995. Mucin biophysics. Annual Review of Physiology 57:635-657.

Bansil R, Turner BS. 2006. Mucin structure, aggregation, physiological functions and biomedical applications. Curr Opin Coll Interf Sci 11:164-170.

Bloomfield VA. 1983. Hydrodynamic properties of mucus glycoproteins. Biopolymers 22:2141-2154.

Cao X, Bansil R, Bhaskar KR, Turner BS, LaMont JT, Niu N, Afdhal N. 1999. pH-dependant conformational change of gastric mucin leads to the sol-gel transition. Biophys J 76:1250-1258.

Cruz Ramos H, Rumbo M, Sirard J-C. 2004. Bacterial flagellines: mediators of pathogenicity and host immune responses in mucosa. Trends in Microbiol 12:509-517.

Davenport K, Keeley FX. 2005. Evidence for the use of silver-alloy-coated urethral catheters. Journal of Hospital Infections 60: 298-303.

DeGroot MH, Schervish MJ. 2002 Probability and Statistics (3rd edition, Addison Wesley, Boston).

Dubolazov AV, Nurkeeva ZS, Mun GA, Khutoryanskiy VV. (2006) Design of mucoadhesive films based on poly(acrylic acid) and hydroxypropyl cellulose. Biomacromolecules, 7: 1637-1643.

Gilbert P, Evans DJ, Evans E, Duguid IG, Brown MRW. 1991. Surface characteristics and adhesion of *Escherichia coli* and *Staphylococcus epidermidis*. J Appl Bacteriol 71:72-77.

Gingell D, Vince S. 1980. Long-range forces and adhesion: an analysis of cell-substratum studies. In: Cell Adhesion and Motility. Curtis A and Pitts J Editors. Cambridge: Cambridge University Press.

Girón JA, Torres AG, Freer E, Kaper JB. 2002. The flagella of enteropathogenic *Escherichia coli* mediate adherence to epithelial cells. Mol Microbiol 42:361-379.

Hancock I, Poxton I. 1988. Bacterial cell surface techniques. Second edition. Wiley-Interscience: Chichester.

Hazen KC. 1989. Participation of yeast cell surface hydrophobicity in adhesion of *Candida albicans* to human epithelial cells. Infection and Immunity 57:1984-1900.

Hobden C, Teevan C, Jones L, and O'Shea P. 1995. Hydrophobic properties of the cell surface of *Candida albicans*: a role in aggregation. Microbiol 141:1875-1881.

Keddie JL. 2001. Structural analysis of organic interfacial layers by ellipsometry. Curr Opin Colloid Interf Sci 6:102-110.

Klotz SA, Drutz DJ, Zajic JE. 1985. Factors governing adhesion of *Candida albicans* species to plastic surfaces. Infection and Immunity 50:97-101.

Landry RM, An D, Hupp JT, Singh PK, Parsek, MR. 2005. Mucin-*Pseudomonas aeroginosa* interactions promote biofilm formation and antibiotic resistance. Mol. Microbiol. 59:142-151.

Mack D, Becker P, Chatterjee I, Dobinsky S, Knoblock J, Peters G, Rohde H, Herrmann M. 2004. Mechanisms of biofilm formation in *Staphylococcus epidermidis* and *Staphylococcus aureus*: functional molecules, regulatory circuits and adaptive responses. Int J Med Microbiol 294:203-212.

MacKay DJ. 2004. Information Theory, Inference, and Learning Algorithms (Cambridge University Press, Cambridge).

Malmsten M, Blomberg E, Claesson P, Carlstedt I, Ljusegren I. 1992. Mucin layers on hydrophobic surfaces studied with ellipsometry and surface force measurements. J Colloid Interface Sci 151:579-590.

Nikonenko NA, Bushnak IA, Keddie JL. 2009. Spectroscopic ellipsometry of mucin layers on an amphiphilic diblock copolymer surface. Appl Spectroscopy 63:889-898.

Park H, Robinson JR. 1987. Mechanisms of mucoadhesion of poly(acrylic acid) hydrogels. Pharm Res 4:457-464.

Patel MM, Smart JD, Nevell TG, Ewen RJ, Eaton PJ, Tsibouklis J. 2003. Mucin/poly(acrylic acid) interactions: a spectroscopic investigation on mucoadhesion. Biomacromolecules 4:1184-1190.

Peppas NA, Huang Y. 2004. Nanoscale technology of mucoadhesive interactions. Adv Drug Delivery Rev 56:1533-1536.

Perez E, Proust JE. 1987. Forces between mica sheets covered with adsorbed mucin across aqueous solution. J Coll Interf Sci 118:182-191.

Prescott L, Harley JP, Klein DA. 1993. Microbiology. 2nd Revised edition. Wm. C. Brown Co.: Oxford.

Richardson H, Lopez-Garcia I, Sferrazza M, Keddie JL. 2004. Thickness dependence of structural relaxiation in spin-cast, glassy polymer thin films. Phys Rev E 70:051805.

Rosenberg M. 1988. Ammonium sulphate enhances adherence of *Escherichia coli* J to hydrocarbons and polystyrene. FEMS Microbiol Lett 25:41-45.

Rutter PR, Dazzo FB, Freter R, Gingell D, Jones G, Kjelleberg S, Marshall K, Mrozek H, Rades-Rohkohl E, Robb I, Silverman M, Tylewska S. 1984. Mechanisms of

adhesion. In: Microbial Adhesion and Aggregation. Marshall KC Editor. Berlin: Springer-Verlag.

Sheehan JK, Oates K, Carlsted I. 1986. Electron microscopy of cervical, gastric and bronchial mucus glycoproteins. Biochem J 239:147-153.

Shi L, Caldwell KD. 2000. Mucin adsorption to hydrophobic surfaces. J Colloid Interface Sci 224:372-381.

Shi L, Ardehali R, Caldwell KD, Valint P. 2000. Mucin coating on polymeric material surfaces to suppress bacterial adhesion. Colloids Surf B 17:229-239

Singh A, Awar M, Ahmed A, Fischman DL, Walinsky P, Savage MP. 2007. Facilitated stent delivery using applied topical lubrication. *Catheterization and Cardiovascular Interventions* 69:218-222.

Strous GJ, Dekker J. 1992. Mucin-type glycoproteins. Crit Rev Biochem Mol Biol 27:57-92.

Sundstrom P. 1999. Adhesion in *Candida albicans*. Curr Opin Microbiol 2:353-357.

Tenke P, Jackel M, Nagy E. 2004. Prevention and treatment of catheter associated infections: myth or reality? EAU Update Series 2:106-115.

Tunney MM, Gorman SP. 2002. Evaluation of a poly(vinyl pyrollidone)-coated biomaterials for urological use. Biomaterials 23:4601-4608.

Vacheethasanee K, Temenoff JS, Higashi JM, Gary A, Anderson JM, Bayston R, Marchant RE. 1998. Bacterial surface properties of clinically isolated *Staphylococcus epidermidis* strains determine adhesion on polyethylene. Journ Biomed Mat Res 42:425-432.

Wardell JN. 1988. Methods for the study of bacterial attachment. In: Methods in Aquatic Bacteriology. Austin B, Editor. Chichester: Wiley.

Wong ES, Hooton TM. 1981. Guidelines for prevention of catheter-associated urinary tract infections. Centers for Disease Control and Prevention. Available from: http://www.cdc.gov/ncidod/dhqp/gl_catheter_assoc.html

Table 1. Thickness of the polymer and mucin films

Sample	pH of mucin solution	Thickness (nm)		
		SiO_2	(co)polymer	mucin
Si/mucin	3	2.3	-	3.5±1.5
Si/mucin	7	2.3	-	4.2±2.1
Si/mucin	10	2.5	-	3.0±2.0
PMMA/mucin	3	2.4	17.4±2.0	3.0±1.2
PMMA/mucin	7	2.5	18.4±2.5	2.6±1.5
PMMA/mucin	10	2.2	17.3±2.2	2.4±1.0
PAA-*b*-PMMA /mucin	3	2.3	20.3±2.0	16.1±2.2
PAA-*b*-PMMA /mucin	7	2.7	18.5±2.3	6.6±1.5
PAA-*b*-PMMA /mucin	10	2.3	18.0±2.2	7.0±1.0

Table 2. Water contact angle measurements on the polymer surfaces before and after soaking in DI-water and after mucin adsorption at pH 7 or pH 3.

Polymer	Contact angle on annealed surface (º)	Contact angle after soaked in DI water (º)	Contact angle on mucin coating	
			Deposited at a pH of 7 (º)	Deposited at a pH of 3 (º)
PMMA	69.4±0.2	71.0±1.2	50.2±4.0	58.4±7.2
PAA-*b*-PMMA	49.1±1.0	40.0±0.8	40.4±1.4	22.6±0.5

Table 3. Cell densities for *E. coli* and *S. Epidermidis* on various surfaces.

	Estimate of the true cell density*, ρ (10^6 cells/cm^2) (% reduction)$^{\infty}$	
Surface	*S. Epidermidis*	*E. coli*
Si	6.90±0.16$^{\perp}$	0.92±0.02$^{\perp}$
Si/mucin	0.90±0.01 (87%)	0.47±0.03 (49%)
PMMA	2.50±0.12	0.91±0.02
PMMA/mucin	0.10±0.01 (96%)	0.20±0.01 (77%)
PAA-*b*-PMMA	0.70±0.02	0.19±0.008
PAA-*b*-PMMA /mucin (pH=7)	0.091±0.009 (87%)	0.030±0.002 (84%)
PAA-*b*-PMMA /mucin (pH=3)	0.050±0.005 (93%)	0.026±0.002 (86%)

* The true cell density, ρ, is the mean of the probability density function in Fig. 2 or Fig. 5

$^{\infty}$The percentages in parentheses for the mucin-coated surfaces are the reductions in cell density when compared to the same surface without mucin.

$^{\perp}$The error is the standard deviation of the probability density functions.

Figure Captions

Figure 1. Microscope images of *S. epidermidis* cells adhering to: a) silicon, b) mucin-coated silicon, c) PMMA, and d) mucin-coated PMMA surface. Scale bar (200μm) applies to all four images.

Figure 2. The probability density function for the true cell density of *S. epidermidis* cells on the surfaces: Si (light purple curve), Si/mucin (Si/m, maroon), PMMA (P, black), PMMA/mucin (P/m, red), PAA-*b*-PMMA (copol, turquoise), PAA-*b*-PMMA/mucin (coated at pH = 7) (copol/m (7), light green) and PAA-*b*-PMMA/mucin (coated at pH = 3) (copol/m (3), blue).

Figure 3. Optical photomicrographs of *S. epidermidis* cells adhering to: a) a PAA-*b*-PMMA film, b) mucin coating cast from a solution with a pH of 7 on PAA-*b*-PMMA, and c) mucin coating cast from a solution with a pH of 3 on PAA-*b*-PMMA. The scale bar (200 μm) applies to all three images.

Figure 4. Optical photomicrographs of *E. coli* cells adhering to: a) silicon, b) mucin-coated silicon, c) PMMA, and d) mucin-coated PMMA surfaces. Scale bar of 200 μm is in all images.

Figure 5. The probability density function for the true cell density of *E. coli* cells on the surfaces: Si (light purple curve); Si/mucin (Si/m, maroon); PMMA (P, black); PMMA/mucin (P/m, red); PAA-*b*-PMMA (copol, turquoise); PAA-*b*-PMMA/mucin (coated at pH = 7) (copol/m (7), light

green); and PAA-*b*-PMMA/mucin (coated at pH = 3) (copol/m (3), blue).

Figure 6. Optical photomicrographs of *C. albicans* cells adhering to: a) silicon, b) mucin-coated silicon, c) PMMA, d) mucin-coated PMMA, e) PAA-b-PMMA, and f) mucin-coated PAA-b-PMMA surfaces. All scale bars are 200 μm.

Figure 7. *C. albicans* cell counts on silicon, PMMA, and PAA-*b*-PMMA before (black bars) and after (gray bars) mucin adsorption.

Figure 8. Correlation between the mucin layer thickness (shown with open triangles, reading on the right axis) and the adherence percentage (left axis) of yeast and bacteria on mucin-coated Si, PMMA, and PAA-b-PMMA. An increase in adhesion is represented above the dashed line, and decreased adhesion is represented below it.

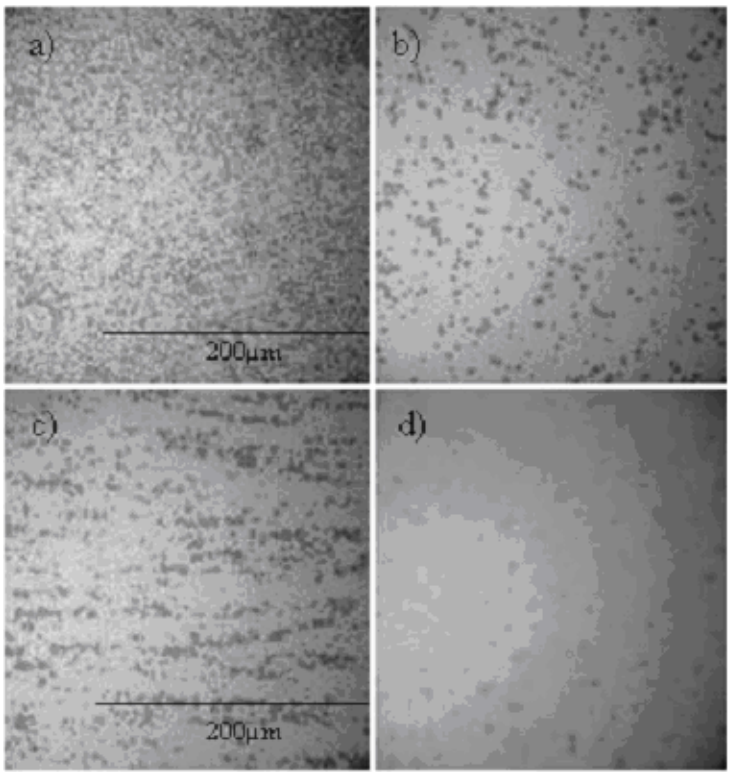

Figure 1. Microscope images of *S. epidermidis* cells adhering to: a) silicon, b) mucin-coated silicon, c) PMMA, and d) mucin-coated PMMA surface. Scale bar (200µm) applies to all four images.

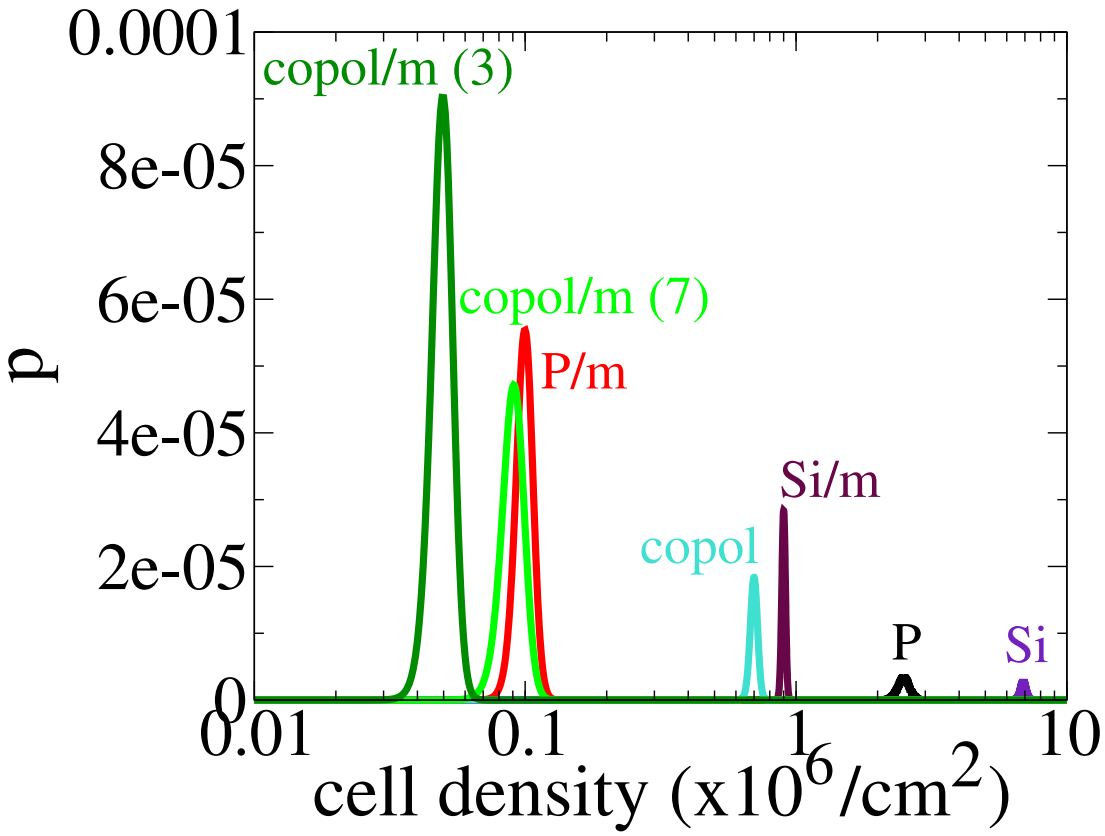

Figure 2. The probability density function for the true cell density of *S. epidermidis* cells on the surfaces: Si (light purple curve), Si/mucin (Si/m, maroon), PMMA (P, black), PMMA/mucin (P/m, red), PAA-*b*-PMMA (copol, turquoise), PAA-*b*-PMMA/mucin (coated at pH = 7) (copol/m (7), light green) and PAA-*b*-PMMA/mucin (coated at pH = 3) (copol/m (3), blue).

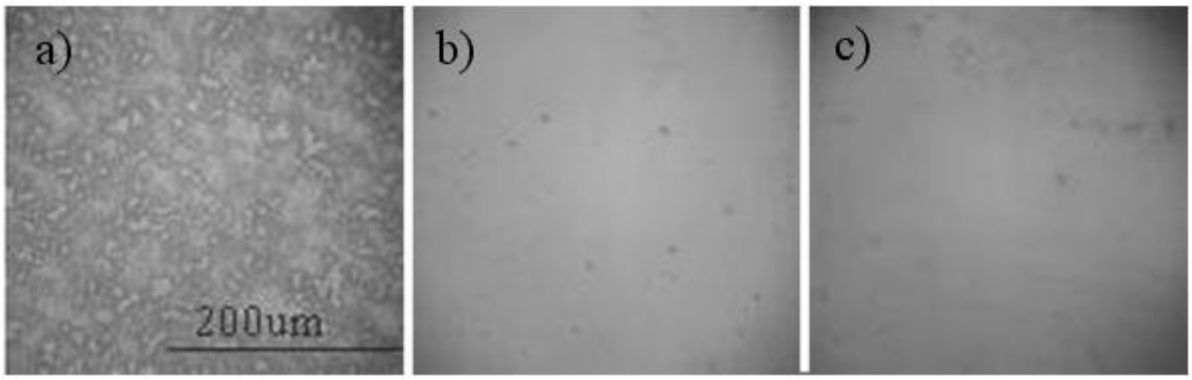

Figure 3. Optical photomicrographs of *S. epidermidis* cells adhering to: a) a PAA-*b*-PMMA film, b) mucin coating cast from a solution with a pH of 7 on PAA-*b*-PMMA, and c) mucin coating cast from a solution with a pH of 3 on PAA-*b*-PMMA. The scale bar (200 μm) applies to all three images.

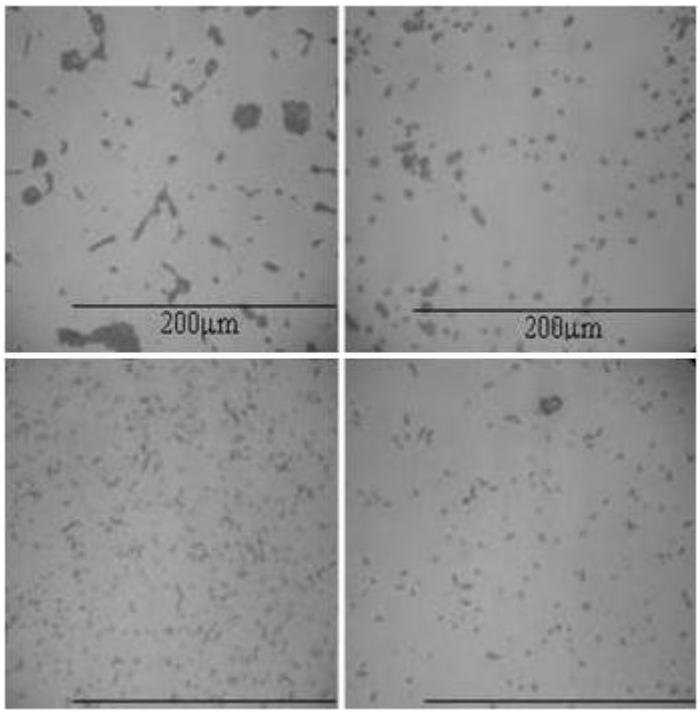

Figure 4. Optical photomicrographs of *E. coli* cells adhering to: a) silicon, b) mucin-coated silicon, c) PMMA, and d) mucin-coated PMMA surfaces. Scale bar of 200 μm is in all images.

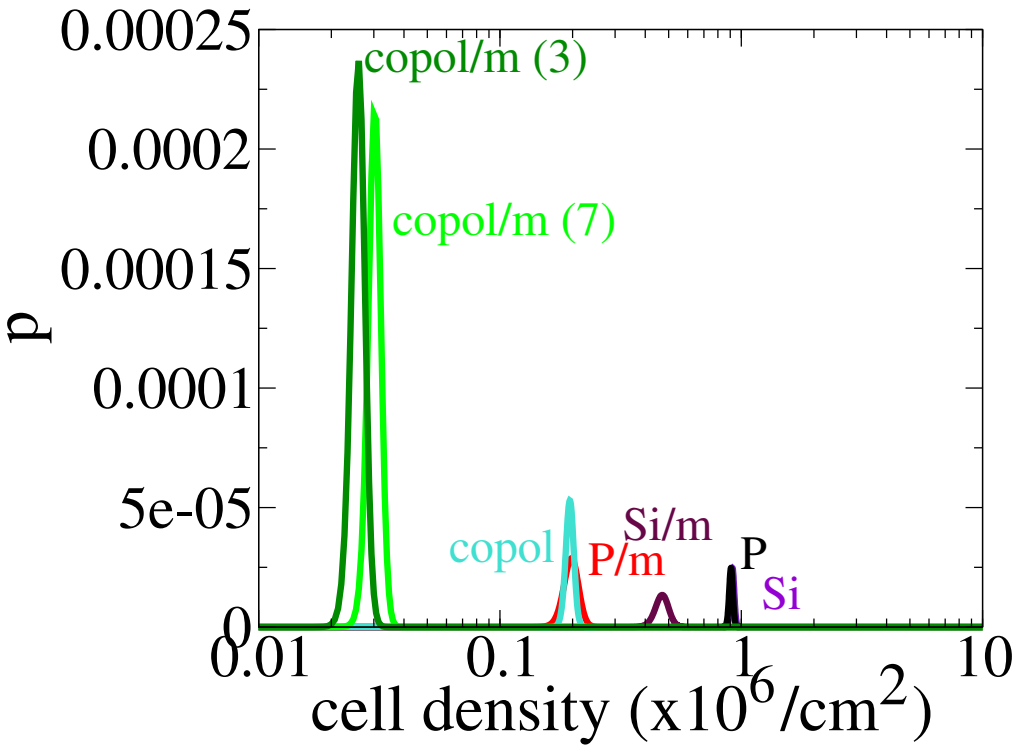

Figure 5. The probability density function for the true cell density of *E. coli* cells on the surfaces: Si (light purple curve); Si/mucin (Si/m, maroon); PMMA (P, black); PMMA/mucin (P/m, red); PAA-*b*-PMMA (copol, turquoise); PAA-*b*-PMMA/mucin (coated at pH = 7) (copol/m (7), light green); and PAA-*b*-PMMA/mucin (coated at pH = 3) (copol/m (3), blue).

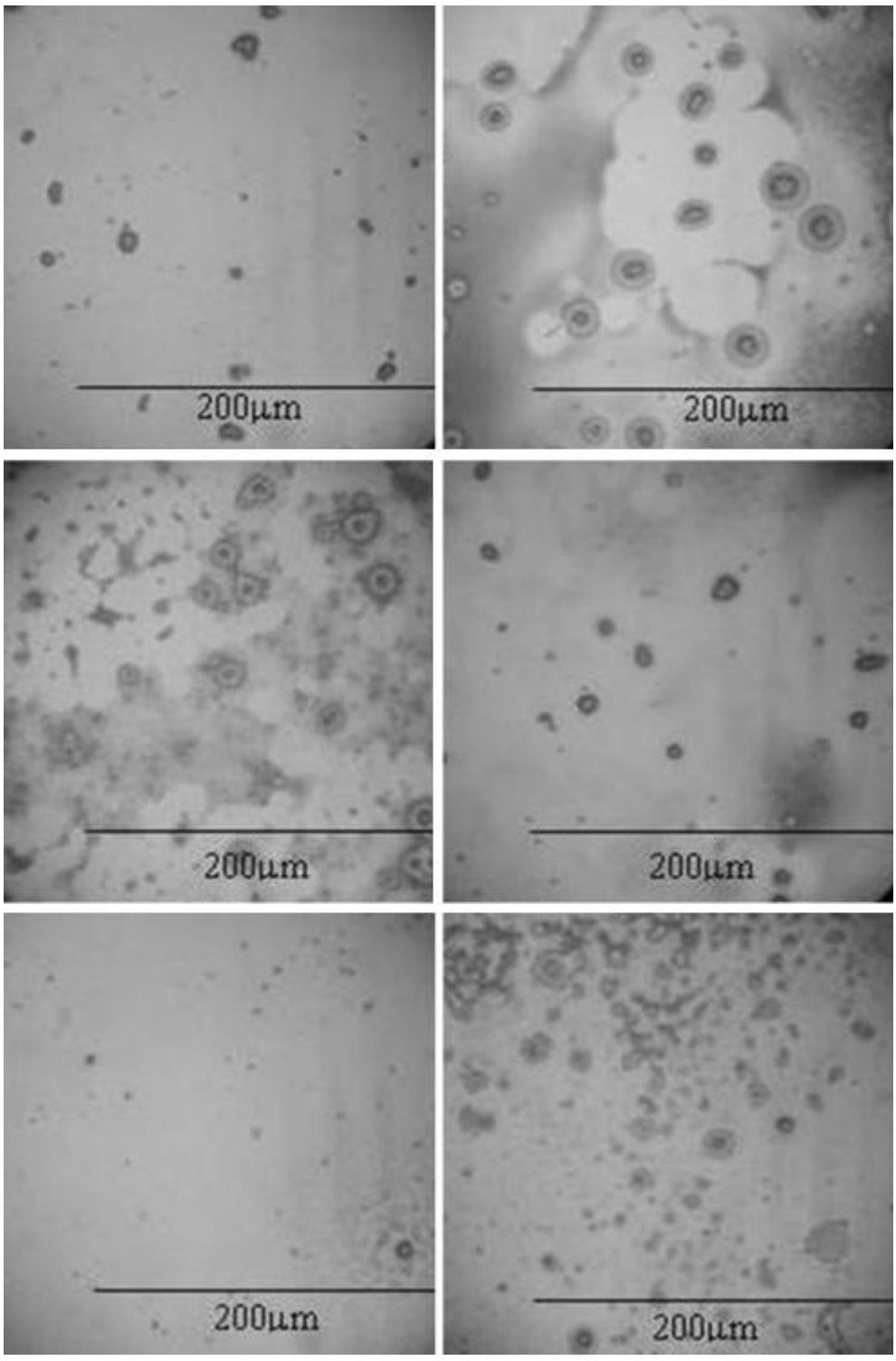

Figure 6. Optical photomicrographs of *C. albicans* cells adhering to: a) silicon, b) mucin-coated silicon, c) PMMA, d) mucin-coated PMMA, e) PAA-b-PMMA, and f) mucin-coated PAA-b-PMMA surfaces. All scale bars are 200 µm.

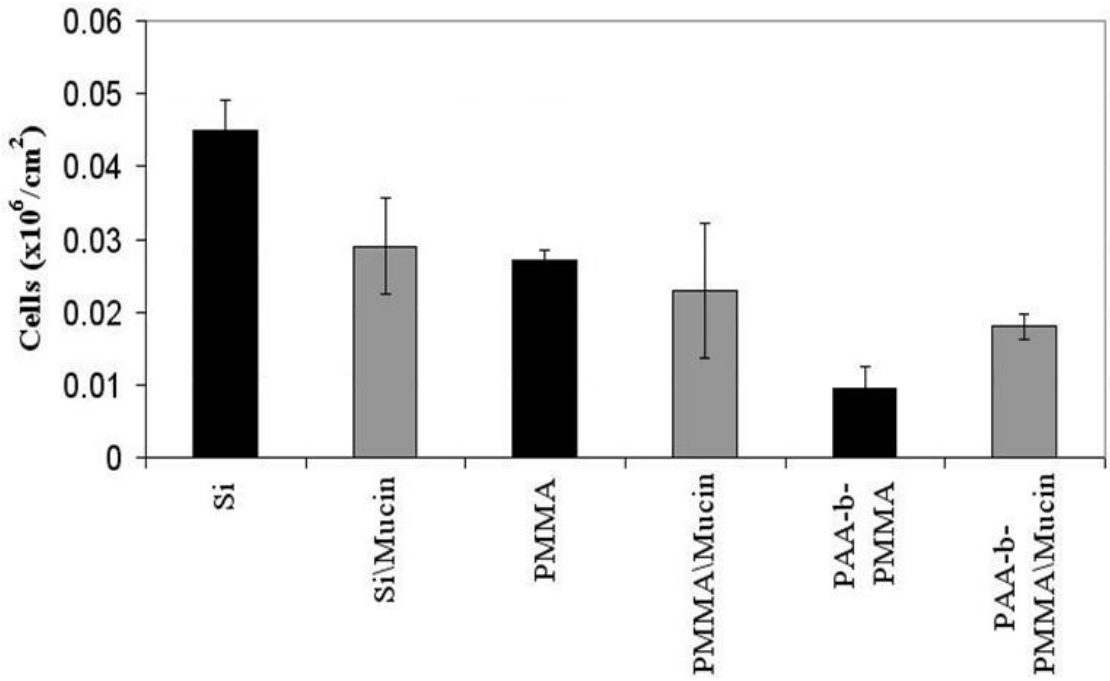

Figure 7. *C. albicans* cell counts on silicon, PMMA, and PAA-*b*-PMMA before (black bars) and after (gray bars) mucin adsorption.

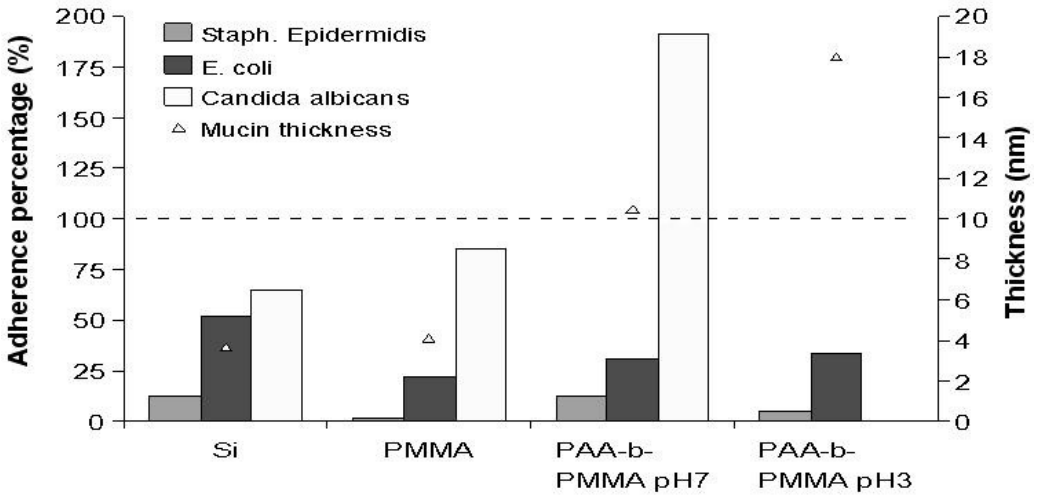

Figure 8. Correlation between the mucin layer thickness (shown with open triangles, reading on the right axis) and the adherence percentage (left axis) of yeast and bacteria on mucin-coated Si, PMMA, and PAA-b-PMMA. An increase in adhesion is represented above the dashed line, and decreased adhesion is represented below it.